

## Propagation and out-coupling of electron-beam excited surface plasmons on gold

R. E. Peale

Department of Physics and School of Optics and Photonics  
University of Central Florida, Orlando FL 32816

O. Lopatiuk, J. Cleary, S. Santos, J. Henderson, D. Clark, L. Chernyak, T. A. Winningham, E. Del Barco

Department of Physics  
University of Central Florida  
Orlando, FL 32816-2455

H. Heinrich

Department of Physics and Advanced Materials Processing and Analysis Center (AMPAC)  
University of Central Florida  
University of Central Florida, Orlando FL 32816

W. R. Buchwald

Air Force Research Laboratory, Sensors Directorate, Hanscom AFB MA 01731

### ABSTRACT

Surface plasmon propagation on gold over 0.1 – 1.6 micrometer distances for plasmon energies in the range 1.6 – 3.5 eV was characterized. Surface plasmons were excited by an electron beam near a grating milled in the gold. The spectra of out-coupled radiation reveal increasingly strong propagation losses as surface plasmon energy increases above 2.8 eV, but little effect in the range 1.6 – 2.8 eV. These results are in partial agreement with theoretical expectations.

### INTRODUCTION

Propagation of electromagnetic signals on metal waveguides via highly-confined, bound electro-magnetic waves known as surface plasmon polaritons (SPP) is central to nano-photonics [1, 2]. Plasmon-electronic integrated circuits (PEIC) have been proposed [3], but the usual optical inputs and outputs for PEIC involve bulky optics. Potentially more compact would be electrical SPP generation and detection, e.g. by electron bombardment using nano-tube field emitters. The spectrum of electron-beam excited SPPs on metals is concentrated at high visible and ultraviolet energies. Although the characteristic propagation length generally decreases with energy for free-electron metals, gold specifically has a propagation length that is expected to remain constant at about 0.3  $\mu\text{m}$  above 2.5 eV (see below). Thus, electron-beam excited, high-frequency SPPs on gold are potentially interesting for nano-scale PEIC applications. Use of a scanning electron microscope (SEM) and cathodoluminescence (CL) to study SPP decay for 1-10  $\mu\text{m}$  propagation lengths at energies below 2.3 eV was recently described [4-6]. This paper reports an independent experiment of the same type, but where sub-micron propagation is observed at SPP energies above 2.8 eV.

## EXPERIMENT

A nominally 470 nm thick layer of gold was e-beam evaporated onto a 5 nm Cr sticking layer on a polished silicon substrate. This thickness is sufficient that the optical constants are those of bulk gold. Using a 30 keV focused gallium-ion beam (FIB), several 20-line gratings were cut in the gold. The Figure 1 inset presents an FIB micrograph of one of the gratings, where all twenty of the 57  $\mu\text{m}$ -long lines appear in the upper part of the image.

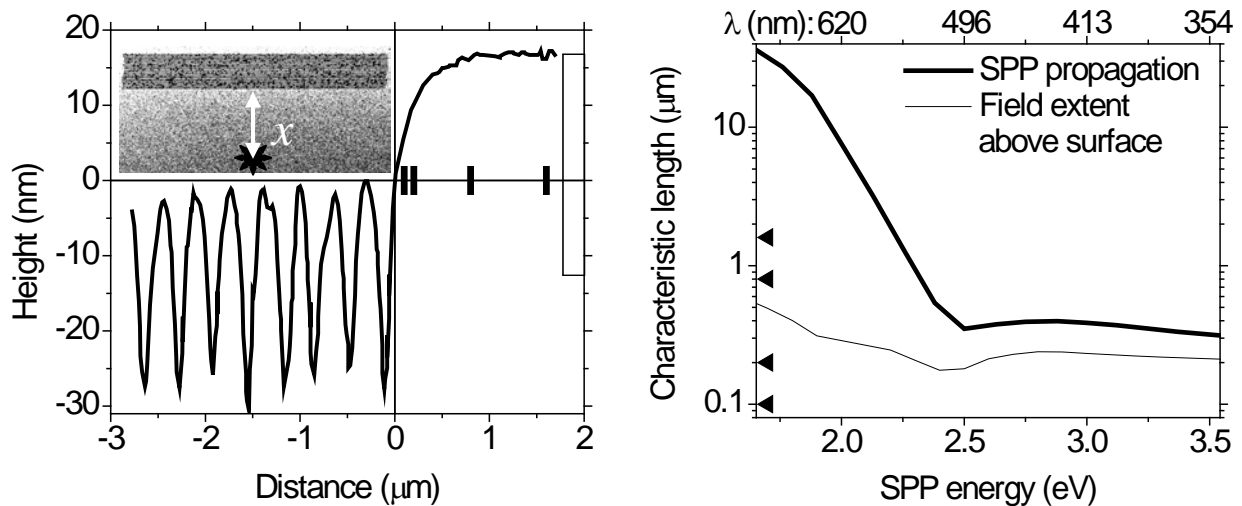


**Figure 1.** (left) Atomic force microscopy line scan of grating on gold film. The inset is a focused ion beam micrograph of the grating. The black star schematically represents the  $\sim 5$  nm diameter electron beam spot (exaggerated for clarity) at a distance  $x$  (also exaggerated) from the rulings. Cathodoluminescence spectra were collected as a function of  $x$ . The bar symbols on the zero line indicate the  $x$ -values probed. The shaded box represents the penetration depth of the surface plasmon fields into the metal

**Figure 2.** (right) Characteristic lengths as a function of SPP energy. The propagation length for SPPs on gold is given by the heavy curve. The light curve is the SPP penetration depth into the air above the surface. The triangle symbols indicate the distances from the grating that SPPs were excited by the electron beam. The tick labeling on the upper border indicates the photon wavelengths for out-coupled SPPs.

Atomic Force Microscopy (AFM) shows that the as-evaporated surface consists of bumps with 1-4 nm height, 50 nm diameter, and  $\sim 50$  nm average separation. The Figure 1 AFM image slice reveals 30 nm groove depths, but the profiles are degraded by the AFM tip size [7, 8]. The grating period is 360 nm. Figure 1 also reveals that the regions between the grooves have been collaterally milled and are lower than the surrounding unstructured gold by about 17 nm.

A scanning electron microscope cathode-luminescence system collects spectra for different electron-beam positions. An off-axis parabolic aluminum mirror collects  $\sim 75\%$  of all light emitted from the vicinity of the excitation. The electron beam transits a 1 mm aperture in the mirror to excite SPPs at the mirror focus. Collection system dimensions sufficiently exceed SPP propagation lengths that SPP out-coupling occurs essentially at the focus.

The Figure 1 inset schematically indicates the e-beam spot at a distance from the grating of  $x$ , where surface plasmons with a certain frequency distribution are excited with efficiency  $< 1\%$  [4, 9]. SPPs propagate away from the excited spot, and those that reach the grating are coupled into free electromagnetic waves with an efficiency that depends on grating geometry [10]. Vertical bar symbols on the zero-line of Figure 1 indicate the actual  $x$ -positions probed.

## THEORETICAL CONSIDERATIONS

The complex SPP wavevector is determined from the complex permittivity  $\epsilon$  of the metal, according to

$$k = (\omega/c)\sqrt{[\epsilon/(1+\epsilon)]}, \quad (1)$$

where  $\omega$  is the angular frequency and  $c$  is the speed of light. Empirical permittivity data for gold [11] were used to obtain the dispersion relation  $\omega$  vs  $\text{Re}[k]$ . Between 2 and 2.5 eV (620-500 nm wavelength), the SPP dispersion curve falls noticeably below the light line  $\omega = c k$ . Above 2.5 eV, rather than leveling off at an SPP resonance frequency as for free-electron metals, the curve for gold doubles back toward the light line while remaining below it. The fundamental condition for SPPs that  $\text{Re}[\epsilon] < 0$  remains valid up to at least 5 eV.

The characteristic propagation length  $L$  for SPP intensity is given by  $L^{-1} = 2 \text{Im}[k]$ . Figure 2 presents calculated  $L$  values using permittivity from [11] over the experimental spectral range, where we find  $0.3 \mu\text{m} < L < 40 \mu\text{m}$ . Above 2.5 eV (below 500 nm optical wavelength),  $L$  is fairly constant at  $\sim 0.3 - 0.4 \mu\text{m}$ . Symbols indicate distances  $x$  probed in the experiment.

SPP fields extend above the surface and penetrate into the gold by amounts

$$L_{\text{Air}} = (c/\omega) / \text{Re}[\sqrt{-1/(1 + \epsilon)}]$$

and

$$L_{\text{Au}} = (c/\omega) / \text{Re}[\sqrt{-\epsilon^2/(1 + \epsilon)}], \quad (2)$$

respectively.  $L_{\text{Air}}$  values in the experimental spectral range are plotted in Figure 2 and fall between 0.2 and 0.6  $\mu\text{m}$ . Values for  $L_{\text{Au}}$  are between 25 and 40 nm, and the shaded box in Figure 1 schematically indicates the value at 3.5 eV. Thus, the comparatively small  $\sim 17$  nm recess of the grating below the surface should not prevent the SPP from feeling the grating, so that out-coupling should proceed in the usual way. However, the spectral efficiency for out-coupling may be very different from that of the gratings in [4-6].

The out-coupling angle  $\theta$  is determined by

$$\text{Re}[k] = (2 \pi/\lambda) \text{Sin } \theta + 2 \pi m/a, \quad (3)$$

where  $m$  is a positive integer. The apparatus collects only  $m = 1$  emission over the spectral range of the experiment. For  $a = 50$  nm, the characteristic length scale of surface roughness, there are no real solutions for  $\theta$  in the experimental spectral range, so that contributions to the background from out-coupling by roughness should be weak.

SPP excitation by electron beams is sharply peaked at the SPP resonance frequency  $\omega = \omega_p/\sqrt{2}$  for free-electron metals [12]. Experiment [13] and simulation [14] reveal two peaks in the electron energy loss spectrum for gold due to SPP generation. These occur near 2.8 and 5.7 eV as indicated by symbols in Figure 3. The SPP resonance frequency determined by  $\epsilon = -1$  [15] corresponds to peaks in the electron energy-loss function for SPP generation  $\text{Im}[-1/(\epsilon + 1)]$  [10], which do occur near 2.8 and 5.7 eV (Figure 3).

Next, theoretical considerations relevant to the analysis of the experimental data are presented. The measured emission spectrum  $I(x, \lambda)$  is

$$I(x, \lambda) = S(\lambda) \{B(\lambda) + D(\lambda) \text{Exp}[-x/L(\lambda)]\}. \quad (4)$$

$D(\lambda)$  is the distribution of surface plasmons at frequency  $\omega$  excited by the electron beam, which is observed (Figure 3) to fall sharply for energies below 2.5 eV to the level of only a few % of the peak value. The ratio of  $I(x, \lambda)$  to  $I(x \gg L, \lambda)$  is

$$R(x, \lambda) = 1 + [D(\lambda)/B(\lambda)] e^{-x/L(\lambda)}. \quad (5)$$

The second term is small compared with unity, and becomes rapidly smaller with increasing  $\lambda$  due to the factor  $D/B$ .  $B(\lambda)$ , which is determined from  $I(x \gg L, \lambda)$  and the known spectrometer response function  $S(\lambda)$ , is usually assumed [4-6] to be independent of  $x$ .

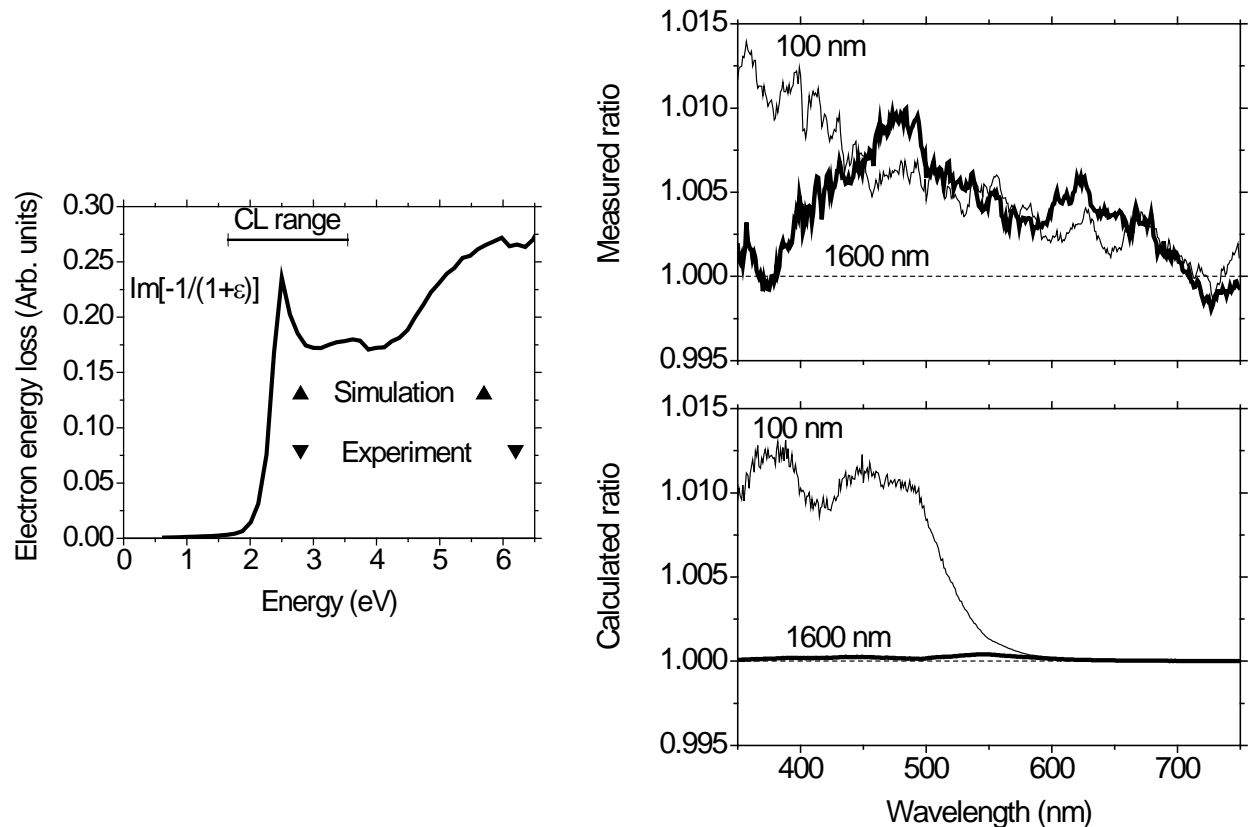


**Figure 3.** (left) Electron energy loss spectrum for generation of SPPs on gold. The symbols represent experimentally observed [13] and simulated [14] energy loss peaks. The curve is the energy loss function calculated from the permittivity. The range of photon energies collected by the cathodo-luminescence experiment is indicated by the horizontal bar.

**Figure 4.** (right) Measured (top) and calculated (bottom) ratios of cathodo-luminescence spectra. Distances of electron-beam excitation spot from the grating out-coupler are indicated.

## RESULTS

Experimental ratios  $I(x, \lambda) / I(1 \text{ mm}, \lambda)$  are presented in the upper part of Figure 4 for two distances  $x$ . At  $x = 100 \text{ nm}$ , the short-wave emission dominates. At  $x = 1600 \text{ nm}$ , the emission for  $\lambda < 450 \text{ nm}$  drops to the level of the background, while the longer wave emission remains strong. The lower part of Figure 4 presents calculated ratios Eq. (5) for the same two distances. The calculated ratios adequately reproduce the observed drop in the values for  $\lambda < 400 \text{ nm}$ . The calculated ratios converge to unity for  $\lambda > 700 \text{ nm}$  as seen in the data. However, the drop with  $x$  between 400 and 700 nm is less rapid, or even non-existent in comparison with the calculated effect.

Figure 5 presents a plot of the experimental ratios for three different wavelengths as a function of distance. The heavy curve is the calculated ratio at 350 nm, and the calculated curves for other wavelengths are similar. At 350 nm, the experimental ratio drops rapidly to unity in fair agreement with the calculation. However, at 450 nm the experimental ratio hardly changes at all, which is significantly different than the calculation.

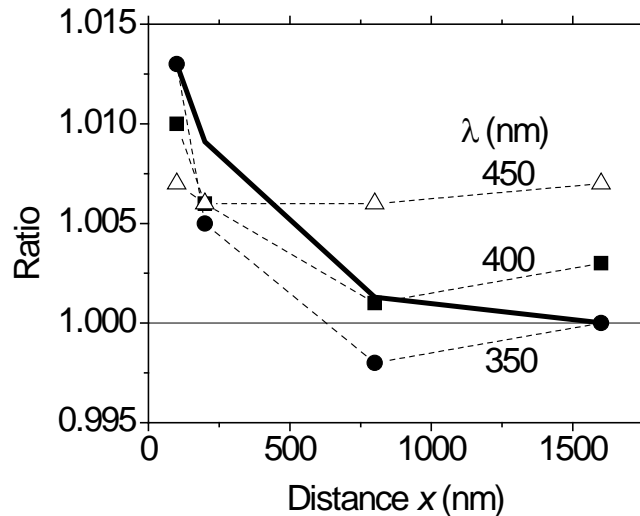


**Figure 5.** Ratios of cathodo-luminescence spectra at three wavelengths (symbols) as a function of the distance of the electron-beam excitation spot from the grating out-coupler. The heavy curve is the calculated ratio for  $\lambda = 350 \text{ nm}$ . Calculated curves for other wavelengths are similar.

## DISCUSSION

Propagation lengths are usually found to be about 2-7 times smaller than predicted by permittivity-based theory [4-6]. If  $L$  is decreased, one finds that the calculated ratio has more of a hump at 500 nm for the larger distances  $x$ , but these calculated ratios also collapse toward unity even more rapidly with  $x$ . Thus, the disagreement in the middle of the spectral range suggests an oversimplification in the formula, especially in the assumption of position independence of the background spectrum  $B$ .

The previous studies describe their background as “significant”[5] or comprising ~75% of the total signal [4]. In our experiment, the differences between spectra near and far from the grating are only about 1%. The origin of the background, and what determines its strength relative to the SPP signal are unclear, though we have argued that SPP out-coupling by surface roughness should be a weak contribution, in contrast to the assumption of [5]. The background may be attributed [4] to d-band emission, dipole radiation originating from incident electrons and

their mirror charges, and contaminant fluorescence, but with unknown relative strengths. To explain the weakness of our SPP signal relative to the background, we suppose that our grating is inefficient at outcoupling SPPs in comparison to those of [4-6]. In [4,6] lines of the grating are raised above the gold surface. In [5], the grating was formed by plasma etching of a Si substrate, later coated in Au, and the tops of the grating bars appear to be level with the gold surface. In contrast, our grating was formed by FIB, which caused the entire grating structure to be sunk by 17 nm below the surrounding surface (Figure 1), giving a discontinuity in height between surface and grating.

In summary, propagation of electron-beam excited surface plasmons on gold was characterized over 0.1 – 1.6  $\mu\text{m}$  distances. The effect of attenuation was observed for surface plasmons with energies in the range 2.8 – 3.5 eV, but not for the lower energies that had been characterized earlier by others. The results are in partial agreement with theoretical expectations. The disagreement is likely due to simplifying assumptions in the calculation.

## ACKNOWLEDGMENTS

The authors wish to acknowledge funding for this work provided by the Air Force Office of Scientific Research Task 06SN05COR and AFRL contract number FA871806C0076.

## REFERENCES

1. M. L. Brongersma and P. G. Kik, *Surface Plasmon Nanophotonics* (Springer, New York, 2007).
2. S. A. Maier, *Plasmonics: Fundamentals and Applications* (Springer, New York, 2007).
3. R. A. Soref, in *Silicon Photonics—The State of the Art*, edited by G. Reed (Wiley, Hoboken, NJ, 2008).
4. M. V. Bashevoy, F. Jonsson, A. V. Krasavin, N. I. Zheludev, Y. Chen, and M. I. Stockman, *Nano Lett.* 6, 1113 (2006).
5. J. T. van Wijngaarden, E. Verhagen, A. Polman, C. E. Ross, H. J. Lezec, and H. A. Atwater, *Appl. Phys. Lett.* 88, 221111-1 (2006).
6. M. V. Bashevoy, F. Jonsson, K. F. MacDonald, Y. Chen, and N. I. Zheludev, *Optics Express* 15, 11313 (2007).
7. J. Aue and J. Th. M. De Hossona, *Appl. Phys. Lett.* 71, 1347 (1997).
8. E. C. W. Leung, P. Markiewicz, and M. C. Goh, *J. Vac. Sci. Technol. B* 15, 181 (1997).
9. H. Raether, in *Physics of Thin Films*, edited by G. Hass, M. H. Francombe, and R. W. Hoffman (Academic, New York, 1977) vol. 9, pp. 145-261.
10. A. V. Krasavin, K. F. MacDonald and N. I. Zheludev, in *Nanophotonics with Surface Plasmons*, edited by V. M. Shalaev and S. Kawata (Elsevier, Amsterdam, 2007), pp. 109-139.
11. P. B. Johnson and R. W. Christy, *Phys. Rev. B* 6, 4370 (1972).
12. R. H. Ritchie, *Phys. Rev.* 106, 874 (1957).
13. J. C. Ingram, K. W. Nebesny, and J. E. Pemberton, *Appl. Surf. Sci.* 44, 293 (1990).
14. Z.-J. Ding and R. Shimizu, *Phys. Rev. B* 61, 14128 (2000).
15. E. A. Stern and R. A. Ferrell, *Phys. Rev.* 120, 130 (1960).